International Conference on Space Optics—ICSO 2018

Chania, Greece

9–12 October 2018

Optical design and characterization of the MOMA laser head flight model for the ExoMars 2020 mission

A. Büttner

M. Ernst

M. Hunnekuhl

R. Kalms

et al.

esa icso proceedings   cnes

Optical design and characterization of the MOMA laser head flight model for the ExoMars 2020 mission

A. Büttner[*a], M. Ernst[a], M. Hunnekuhl[a], R. Kalms[a], L. Willemsen[a], P. Weßels[a], D. Kracht[a],
J. Neumann[a], the MOMA laser team[a,b]
[a]Laser Zentrum Hannover e.V., Hollerithallee 8, 30419 Hannover, Germany
[b]Max Planck Institute for Solar System Research, Justus-von-Liebig-Weg 3, 37077 Göttingen,
Germany

*a.buettner@lzh.de; phone 0049 511 2788 540; fax 0049 511 2788 100; www.lzh.de

ABSTRACT

A space-qualified flight model of a pulsed ultraviolet (UV) laser has been developed for the Mars Organic Molecule Analyzer (MOMA) instrument of the ExoMars 2020 mission. The design is based on a passively Q-switched Nd:Cr:YAG laser oscillator with subsequent two-stage frequency quadrupling. It emits nanosecond pulses with an energy tuneable between 13 µJ and 130 µJ at a wavelength of 266 nm.

Considering its small physical dimensions and weight, the interior of the laser head is rather complex. Besides the aforementioned infrared oscillator and frequency conversion stage it contains the pump optics, two wavelength division assemblies within main beam path, a complex monitoring stage including two photodiodes for pulse energy measurement, a beam shaping setup and a deflection unit for fine adjustment of the beam pointing towards the sample location within the instrument. Most of the laser head is enclosed in a hermetically sealed housing, while the deflection unit is sealed separately. Both volumes are filled with 1 bar of dry, filtered air.

Keywords: Passively Q-switched laser, diode-pumped laser, space-qualified laser, ultraviolet laser, 266 nm laser, ExoMars, MOMA.

1. INTRODUCTION

The MOMA instrument onboard the ESA/Roscosmos ExoMars rover (to be launched in 2020) will be employed to seek for signs of past or present life on Mars through the analysis of the molecular, primarily organic, composition of acquired samples on the ExoMars rover [1] [2]. The instrument includes a pulsed UV laser head (LH) acting as an excitation source for the mass spectrometer (MS) subsystem. MOMA is equipped with two different operational modes. Martian soil samples, obtained by a drill from up to 2 m depth and crushed thereafter, are heated in small ovens in order to induce evaporation and/or pyrolysis of volatile compounds. These are separated by the included gas chromatograph (GC) and then analyzed individually with the mass spectrometer (GCMS mode). For the second operational mode the samples are directly irradiated by intense UV laser pulses to get access to non-volatile compounds. Following prompt laser desorption (LD) into the gas phase, the produced ions are directly sent to the MS without further GC separation (LDMS mode).

The MOMA LH will be the first 266 nm laser in space. During the course of the project it has undergone several design iterations and adaptions to changing performance specifications. For example, the maximum energy specification has been reduced significantly while an energy tuning scheme has been added, which is crucial to adapt for varying requirements from more or less sensitive samples.

The final flight model (FM) design delivers UV pulses at a wavelength of 266 nm with an output energy of up to 130 µJ and a pulse duration of 1.3-1.5 ns focused to a spot of 400 µm diameter at the sample position within the instrument. The output energy is tunable to about 10% of the maximum value. Bursts of up to 50 pulses at an intra-burst repetition rate of 100 Hz and an average repetition rate of 2 Hz are emitted.

In this paper we will present the compact and, considering the stringent mass and volume restrictions, rather complex optical design of the MOMA LH FM together with performance data.

2. OPTICAL CONCEPT

2.1 Overview

The MOMA laser system consists of two main components: the laser pump unit (LPU) and the LH, see Figure 1.
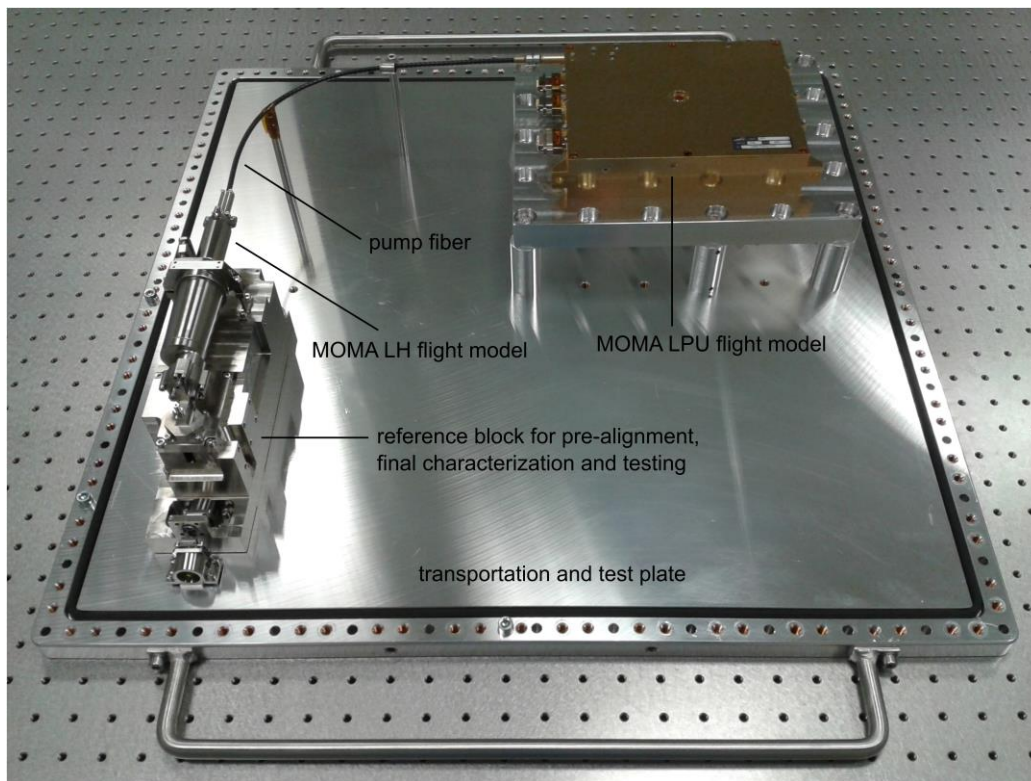

Figure 1. MOMA LH (bottom left) and LPU (top right) on a transportation and test plate, connected with pump fiber (inside black protection tube).

The LPU, which is provided by the Max Planck Institute for Solar System Research (MPS - Göttingen, Germany), contains a fiber-coupled pump diode, as well as the corresponding electronics to operate the laser system. The modular concept with an external pump source allowed for a more simplified and compact setup of the LH itself together with the possibility of a flexible accommodation of the system within the so called analytical lab drawer (ALD) of the ExoMars rover where all the scientific instruments are located. The LH subassemblies are packaged in a hermetically sealed housing which contains the pump optics, a passively Q-switched IR-oscillator, two frequency conversion crystals, a complex monitoring stage for pulse energy measurement, a beam shaping telescope as well as a deflection and alignment unit. The optical concept of the MOMA LH including labelling of its sub-assemblies and optical components is shown in Figure 2.

The complex optical and mechanical design is realized within an envelope of less than 220x57x45 mm³ and has a total mass of less than 220g. Most optics are 4 mm in diameter as a compromise between size, handling and mechanical mounting.
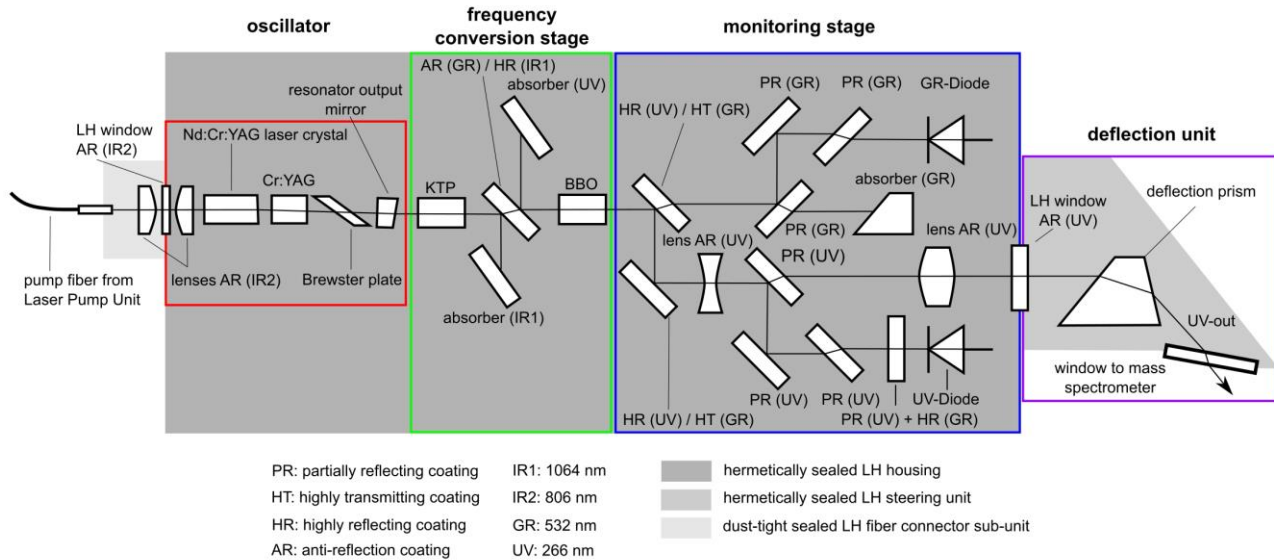
Figure 2. Optical concept of the MOMA LH consisting of four sub-assemblies: oscillator (including pump optics), frequency conversion stage (including beam cleaner), monitoring stage (including beam shaping telescope) and deflection unit.

2.2 Laser pump unit and pump concept

The separate LPU contains a fiber-coupled, temperature stabilized 806 nm pump diode module (PDM), as well as the corresponding power electronics for the PDM. Furthermore, it is equipped with four temperature control circuits for the PDM (one) and the LH (three), photodiode signal detection circuitry for optical measurement of the LH performance as well as the command interface towards the MOMA instrument.

Special to the design of the integrated PDM is its redundancy feature of two separate diode stacks being incorporated into one module. During nominal laser operation, both stacks are operated in parallel at reduced current in favor of an extended lifetime. In case of failure of one diode stack, the other stack can be operated at increased current to fully compensate the defect. Even in single-stack operation the required current is well below the specified maximum value.

The PDM has been designed to deliver pulses with a peak power of up to 160 W and up to 300 μs pulse duration. During the course of the project a modification of the initial oscillator design led to a decreased pump peak power (and pulse energy) requirement. For the FM typically 65 W of peak power are required to emit laser pulses after approximately 140 μs of pump duration ($\approx$ 9 mJ pump energy at 806 nm).

For the science runs of the MOMA instrument the LPU and consequently the UV LH can be operated in a special burst mode. Up to 50 pulses are emitted at 100 Hz repetition rate, while the inter-burst pause is adapted to maintain a maximum average repetition rate of 2 Hz.

Fiber-coupling through a 4 m long fiber, most of which is elliptically coiled inside the LPU housing, ensures an optimum homogenization of pump light both spatially and with respect to polarization. The fiber output is delivered towards the oscillator via two aspheric, radiations hard pump lenses (made of LaK9G15 glass) for longitudinal pumping with an optimized overlap of pump beam and laser mode.

2.3 IR oscillator

The laser oscillator is based on an Nd:Cr:YAG crystal as the active medium (Cr^{3+} co-doping for radiation hardness [3]). The front side of the laser crystal is highly transmissive (HT) coated for the pump wavelength and highly reflective (HR) for the laser wavelength of 1064 nm, thus replacing a separate resonator mirror. The back side of the crystal is anti-reflective (AR) coated for 1064 nm.

Pulse generation is achieved by passive Q-switching with a Cr^{4+}:YAG saturable absorber crystal (AR coated for 1064 nm). This approach enables a short pulse duration in the nanosecond range while being simple, requiring low mass and no additional (high voltage) electronics as compared to active Q-switching schemes. Polarization stabilization, which

is crucial for subsequent resonator-external frequency conversion, is achieved by the <110> crystal cut of the saturable absorber. Its anisotropic transmission behavior provides basic polarization stabilization along the crystal axis exhibiting the lowest loss/highest initial transmission [4]. However, possible depolarization effects due to mechanical clamping of both crystals inside the oscillator can still limit the overall polarization stability. Consequently, an additional Brewster window is utilized to provide further loss at the orthogonal polarization axis. A partially reflective output coupler concludes the oscillator sub-assembly (see Figure 2).

Compared to early prototype models, the FM oscillator design has been optimized with respect to pulse energy stability. Wedged components, namely laser crystal and output coupler, reduce sub-resonator effects from multiple plane-parallel surfaces inside the oscillator [5]. Furthermore, the oscillator sub-assembly is temperature stabilized in order to achieve reproducible output parameters under varying environmental temperatures. Considering the maximum operational environmental temperature on Mars of +25 °C, a heat-only concept with space-qualified temperature sensors (Intersil) and Kapton foil heaters (Minco) is employed.

2.4 Frequency conversion stage and energy tuning

Following the infrared oscillator, the frequency conversion stage (FCS) contains two nonlinear crystals. A KTP crystal (Potassium titanyl phosphate, $KTiOPO_4$, 3 mm long) yields 532 nm radiation via second harmonic generation of 1064 nm (type II phase-matching, eoe-process). A BBO crystal (Beta-Barium Borate, $\beta\text{-}BaB_2O_4$, 2 mm long) provides another frequency doubling step from 532 nm to 266 nm (type I phase-matching, ooe-process).

The frequency conversion stage is thermally decoupled from the oscillator setup and independently temperature stabilized to achieve reproducible output energies over a wide range of environmental conditions. A variation of the output energy is realized via temperature tuning of the frequency conversion stage, i.e. detuning of the conversion crystals from the near-optimum phase-matching condition at the nominal operating temperature. With this approach the output energy can be reduced to approximately 10 % of its maximum value.

2.5 Beam cleaner

In between the two frequency conversion crystals a dichroic mirror - referred to as beam cleaner - filters out the residual 1064 nm radiation to reduce the fluence on the following optics. Although both nonlinear crystals are AR coated for the corresponding input and output wavelengths, any residual UV back-reflection from the output side of the BBO can be very critical for the KTP, as it is highly absorbing at 266 nm. Therefore the back side of the beam cleaner is HR coated for 266 nm and anti-reflective for 532 nm to filter out any UV radiation on the path back to the KTP. Any unconverted radiation at 1064 nm and the small back-reflection at 266 nm are dumped into Brewster-cut absorber optics on both sides of the beam cleaner mirror.

2.6 Beam shaping and monitoring stage

Right behind the BBO crystal two dichroic mirrors, which are HR coated for 266 nm and highly transmitting at 532 nm, provide pre-alignment capabilities of the output beam towards the following telescope and filter out the undesired radiation at 532 nm. The main portion of the unconverted signal is dumped into an absorber optic behind the first dichroic mirror.

In the UV beam path after the second dichroic mirror an expansion lens as part of a two-lens telescope is mounted. On the one hand, the telescope provides beam shaping to the desired spot size of about 400 µm on the target. On the other hand, a lateral adjustment of the telescope's focusing lens allows for further alignment of the output beam direction. The beam diameter is slightly converging towards the sample with the focus being a few centimeters behind the target plane.

A complex monitoring stage (see details in Figure 2) comprises a photodiode for the measurement of the UV output energy as well as a second backup diode that uses the residual 532 nm signal to detect pulse emission and to measure the pulse release time of the oscillator. The optical signals are guided towards the corresponding photodiodes via various mirrors and attenuators with tailored dielectric coatings. New to the FM are coating designs which ensure optimum suppression of signals from other wavelengths present inside the LH (residual pump light at 806 nm as well as 532 nm in the path of the UV photodiode). They provide adequate attenuation to the desired signal levels and effectively avoid interferences between reflections from multiple plane-parallel surfaces (etalon-effects) for optimum measurement accuracy. The UV pulse energy monitoring provides valuable information about the status of the LH as well as a means for precise correlation between the output energy of the LH and the ion count generated by the MS.

2.7 Housing and beam deflection unit

The LH is enclosed in a laser-welded, hermetically sealed housing. AR coated sapphire substrates, brazed to titanium frames and then welded to the housing structure, serve as input and output windows for pump radiation and output signal. The laser housing is filled with dry synthetic air with minimized hydrocarbon content and a dew point < -70 °C. The significant O_2 content allows for an efficient suppression of LIC effects on coatings within the LH [6]. An additional Helium content of 1 % enables leak testing after final sealing of the LH housing.

Behind the output window a pressurized and sealed beam deflection unit, filled with dry air at atmospheric pressure, is mounted. The integrated fused silica prism provides the required deflection of the UV beam towards the sample location within the MOMA instrument. The emitted light is p-polarized relative to the entrance and exit surface of the prism as well as the following fused silica window which acts as a seal between the beam deflection unit of the LH and the adjacent sample zone inside the instrument. The UV beam impinges on both optics at Brewster's angle ensuring minimum losses while reducing the risk of laser induced damage by avoiding four additional AR coatings in an area of increased laser fluence.

Before final sealing of the deflection unit, an adjustment of the position and tilt of the prism allows for a precise alignment of the laser beam with respect to both the sample surface and the ion guide of the mass spectrometer.

3. CHARACTERIZATION AND PERFORMANCE

The initial MOMA oscillator design [5] was capable of delivering IR pulses with approximately 2 mJ of pulse energy with a pulse release time of typically 150-200 µs (time delay measured from the beginning of the pump pulse to the emission of the laser pulse; 100-120 W peak pump power; 1 or 2 Hz operation during assembly and testing). After a reduction of the required UV output energy of the LH the oscillator design was adapted by the use of a saturable absorber with a higher initial transmission. This results in a reduction of the IR output energy to 1.1 mJ with a release time of 140 µs at 65 W of peak pump power. The beam profile of the FM oscillator is slightly elliptical with a roundness factor of 0.95 (see Figure 3). The pulse duration, measured with an ultrafast photodiode and a fast oscilloscope, is 1.6-1.7 ns.
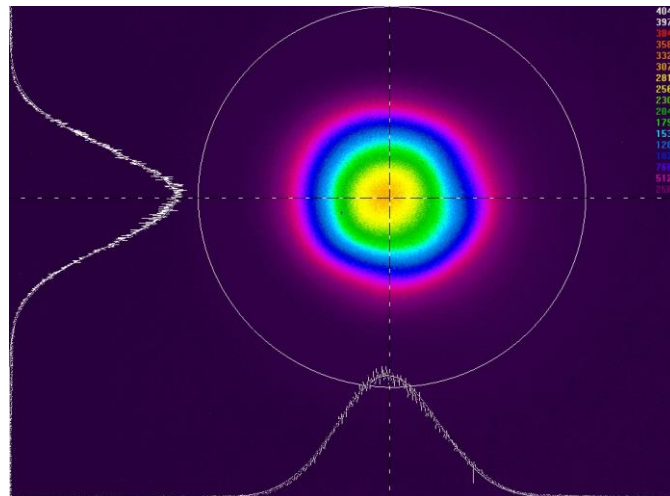

Figure 3. Spatial beam profile at 1064 nm and 1.1 mJ pulse energy from IR oscillator.

Behind the first frequency doubling a pulse energy of 0.6 mJ at 532 nm was achieved for optimum alignment of the KTP crystal (1 Hz operation during assembly), which corresponds to a conversion efficiency of ≈ 55%. As this is slightly more than required to generate the desired amount of UV output and to achieve a higher safety margin with respect to the damage threshold of the following coatings, the angle of the KTP was slightly detuned for the final alignment to generate about 0.5 mJ at 532 nm. The beam profile (see Figure 4) is slightly elliptical analogously to the output from the oscillator.
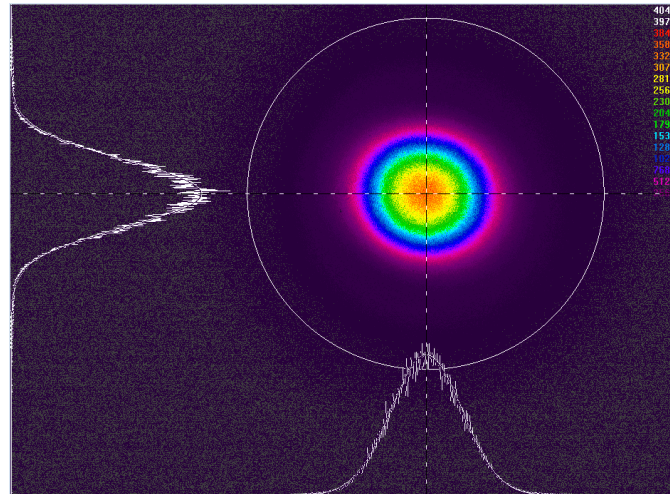
Figure 4. Spatial beam profile at 532 nm and 0.5 mJ pulse energy behind the KTP.

After the second frequency doubling a pulse energy of 160-170 µJ at 266 nm was achieved for optimum alignment of the BBO, which corresponds to a conversion efficiency from 532 nm to 266 nm of ≈ 33 %. To achieve the desired output energy of 130-140 µJ the BBO crystal was slightly detuned analogously to the alignment of the KTP crystal.

The UV beam profile was measured indirectly with a special 1:1 imaging UV-converter device attached to the CCD camera. The calibrated fluorescence image of the laser beam behind the BBO and the dichroic mirrors, but without the beam shaping telescope, is shown in Figure 5 (left). The beam profile is slightly more elliptical (roundness factor 0.76) than the 532 nm input, which can be attributed to the spatial walk-off inside the BBO crystal.

Pulse durations of 1.3-1.5 ns were measured over a wide temperature tuning range of the frequency conversion stage (35 °C to 55 °C), see Figure 5 (right).
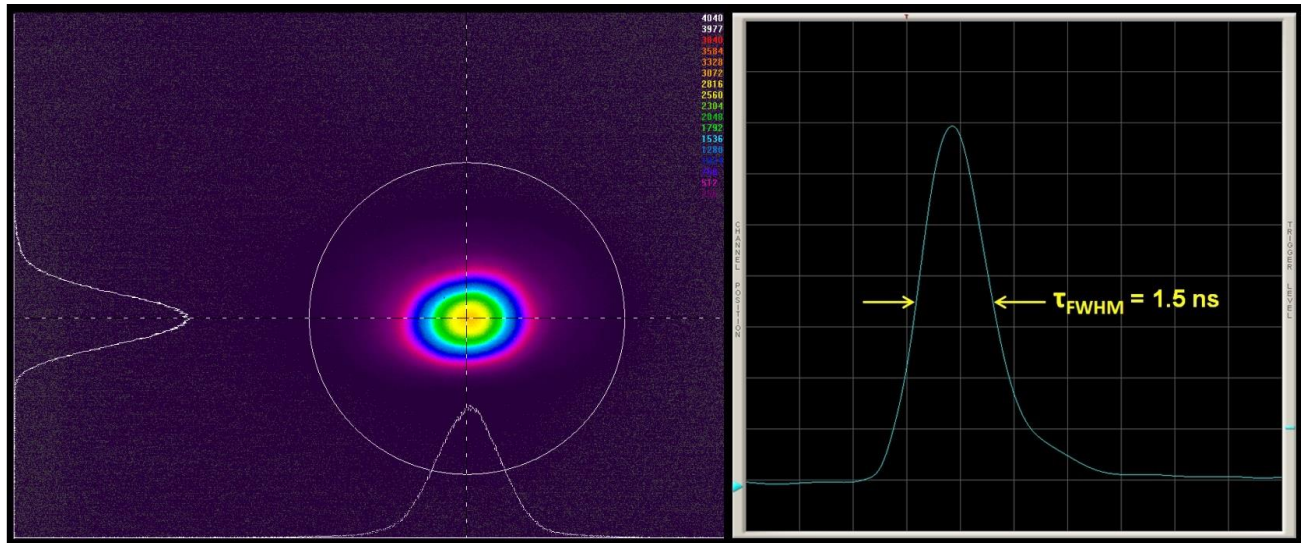

Figure 5. Spatial beam profile at 266 nm and 132 µJ pulse energy (left) and typical temporal pulse profile (right).

The beam profile was also measured behind the beam shaping telescope in a representative distance from the LH reflecting the target location in the instrument. However, this measurement had to be performed before the final assembly of the LH into its sealed housing as the presence of the deflection unit does not provide sufficient clearance for the required measurement setup. In the following Figure 6 two beam profiles are shown that have been taken at different temperatures of the frequency conversion stage (T_{FCS}), corresponding to laser pulse energies of 135 µJ (T_{FCS} = 35 °C) and 12 µJ (T_{FCS} = 55 °C).
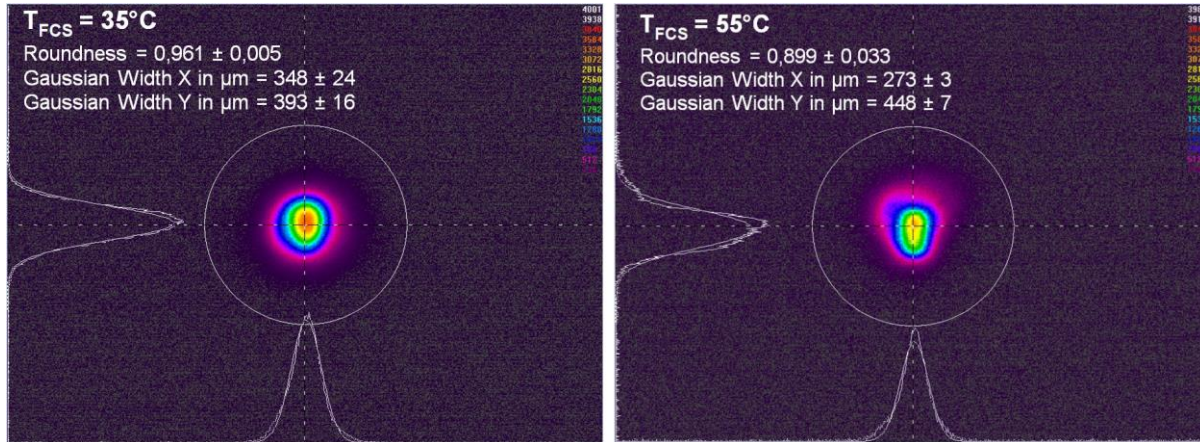
Figure 6. Spatial beam profiles at 266 nm at target distance for two different FCS tuning temperatures (T_{FCS} = 35 °C and T_{FCS} = 55 °C).

During LDMS science runs the LH is operated in burst mode with an intra-burst repetition rate of 100 Hz and a maximum pulse number of 50 per burst. However, typically only a few laser pulses are required to achieve the desired ion count measured by the MS. As compared to continuous 1 or 2 Hz operation, which is usually utilized during assembly and general testing of the LH, slightly differing output energies as well as some characteristic energy dynamics occur during burst operation. Thermal dynamics due to pump light absorption lead to an energy gradient within each burst. To minimize this energy variation, which may be critical for certain sensitive samples, a pre-pulsing scheme is utilized. A defined number of pump pulses that are slightly shorter than the actual release time are fired at the beginning of each burst of pulses. These pump pulses are too short for pulse emission from the oscillator but provide pre-heating of the laser crystal. As a consequence, the most prominent energy deviations at the beginning of each burst are no longer present and the energy gradient is reduced [5].

The following Figure 7 shows a typical energy tuning curve of the LH for burst operation with a fixed number of three pre-pulses (PP) and varying number of 1 to 20 main pulses (MP) per burst. In this example the temperature of the frequency conversion crystals was varied from 35 °C up to 59 °C, corresponding to an energy reduction to well below 10 µJ. At each temperature the average energy per burst, also averaged over several bursts, is given. A variation of the number of main pulses only shows a slight influence on the average output energy of the LH.
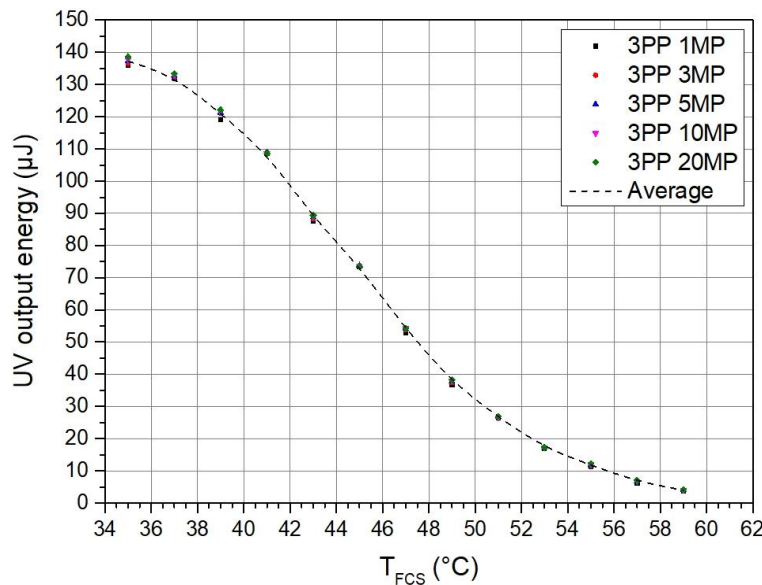

Figure 7. Tuning curve: UV output energy as a function of the frequency conversion stage temperature (T_{FCS}) in burst mode for a varying number of main pulses (MP) per burst.

4. SUMMARY AND OUTLOOK

The MOMA LH flight model delivers nanosecond UV laser pulses at 266 nm wavelength with an energy tuneable between 13 µJ and 130 µJ and a pulse duration of 1.3-1.5 ns. Precise alignment of the laser beam with respect to both the sample surface and the ion guide of the mass spectrometer is achieved by the integrated beam deflection unit. A pulse energy monitoring allows for a correlation between the laser pulse energy and the ion count generated by the instrument.

Following the development and assembly of several LH prototype models the final flight model has undergone an extensive functional and environmental test campaign at MPS. After successful completion of this qualification campaign the MOMA LH has been successfully integrated to the MOMA mass spectrometer flight model at NASA's Goddard Space Flight Center (GSFC - Greenbelt, MD, USA).

Environmental and full functional testing under Mars atmospheric conditions and representative thermal cases has also been successfully completed with the overall MOMA laser desorption mass spectrometer (MOMA LDMS) including the MOMA LH at GSFC.

The next milestone on its way to Mars is the integration of the overall MOMA instrument into the analytical lab drawer (ALD) structure, carrying several scientific instruments within the interior of the ExoMars rover.

5. ACKNOWLEDGEMENT

REFERENCES

[1] Goesmann F. et al., "The Mars Organic Molecule Analyzer (MOMA) Instrument: Characterization of Organic Material in Martian Sediments", Astrobiology, vol. 17 (6 and 7), 655 – 685 (2017)

[2] Vago J., Westall F., Pasteur Instrument Teams, Landing Site Selection Working Group, and other Contributors, "Habitability on Early Mars and the Search for Biosignatures with the ExoMars Rover", Astrobiology, vol. 17 (6 and 7), 471 – 510 (2017)

[3] Glebov B. L. et al., "Improved Hardness of Single-Crystal Nd^{3+}:YAG to Ionizing Radiation via Co-Doping with Cr^{3+}", IEEE Transactions on Nuclear Science, vol. 59 (3), 612 – 618 (2012)

[4] Yoichi Sato and Takunori Taira, "Model for the polarization dependence of the saturable absorption in Cr^{4+}:YAG," Opt. Mater. Express **7**, 577-586 (2017)

[5] Kolleck C., Büttner A., Ernst M., Hunnekuhl M., Hülsenbusch T., Moalem A., Priehs M., Kracht D., Neumann J., "Enhancement of the design of a pulsed UV laser system for a laser-desorption mass spectrometer on Mars", Proc. SPIE 10564, International Conference on Space Optics - ICSO (2012)

[6] Wernham D., Alves J., Pettazzi F., Tighe A. P., "Laser-induced contamination mitigation on the ALADIN laser for ADM-Aeolus", Proc. SPIE 7842, Laser-Induced Damage in Optical Materials: 2010, 78421E (2010)